This is a preprint, the final version is subject to change, of the American Mineralogist (MSA)
Cite as Authors (Year) Title. American Mineralogist, in press.
(DOI will not work until issue is live.) DOI: http://dx.doi.org/10.2138/am.2014.4502

Revision 1

Behavior of gold in a magma at sulfide-sulfate transition: Revisited

Botcharnikov, R.E.[1], Holtz, F.[1], Mungall, J.E.[2], Beermann, O.[1,3], Linnen, R.L.[4], Garbe-Schönberg, D.[3],

[1] *Institut für Mineralogie, Leibniz Universität Hannover, Callinstr. 3, D-30167, Hannover, Germany*

[2] *University of Toronto, Department of Earth Sciences, 22 Russell St., Toronto Ontario, M5S 3B1, Canada*

[3] *Christian-Albrechts-Universität zu Kiel, Institut für Geowissenschaften, Ludewig-Meyn-Str. 10, 24118 Kiel, Germany*

[4] *Department of Earth Sciences, BGS 1000B, University of Western Ontario, London, ON, N5A 5B7, Canada*

e-mail: r.botcharnikov@mineralogie.uni-hannover.de

ABSTRACT

We have investigated experimentally the partitioning of Au between solid and liquid sulfide phases and basaltic melts at 200 MPa, at redox conditions close to the sulfide-sulfate transition, over temperatures between 1050 and 1200 °C which span the monosulfide solid solution (MSS) - sulfide liquid (SuL) solidus. The measured MSS/basalt partition coefficient of Au ($D^{\text{MSS-sil}}_{\text{Au}}$) is about 100-200, whereas the partition coefficient of sulfide liquid/basalt ($D^{\text{SuL-sil}}_{\text{Au}}$) is approximately ten times larger at 2200. Although we find that temperature, pressure, and oxygen fugacity (fO_2) exert relatively weak controls on Au partitioning, they exert major indirect influences on Au behavior by controlling the identity of the condensed sulfide phase and by affecting S solubility. These observations have important implications for the behavior of Au in the processes of partial melting in the mantle and magma crystallization in the crust. The occurrence of natural magmas with elevated concentrations of Au and presumably other highly siderophile and chalcophile elements requires predominance of MSS over SuL in the source or/and oxidizing conditions close to or above the sulfide-sulfate transition in the magma.

Running Title: Behavior of Au in a magma

Key words: gold, sulfur, sulfide, solubility, partitioning, enrichment, magma, basalt

INTRODUCTION

Sulfide liquid (SuL) and monosulfide solid solution (MSS), are key phases that dominate the behavior of highly siderophile elements (HSE) such as Au during magma generation and evolution. It is therefore generally thought that Au-rich magmas cannot form in the presence of residual sulfide in their mantle sources unless it is removed from the source by high degrees of melting (Hamlyn et al. 1985; Solomon 1990), by melting at fO_2 above that of the oxidation reaction that replaces sulfide with sulfur oxide (SSO buffer; Mungall 2002), or by melting at moderately oxidizing conditions (Mungall et al. 2006; Botcharnikov et al. 2011) where the presence of sulfate vastly increases the solubility of sulfur and hastens its exhaustion from the mantle restite. Experiments at reducing conditions and high temperatures have determined that the sulfide/silicate partitioning coefficient $D^{\text{sulfide-silicate}}_{\text{Au}}$ is as high as 10,000 (e.g., Fleet et al. 1999). Botcharnikov et al. (2011) measured much smaller $D^{\text{sulfide-silicate}}_{\text{Au}}$ of only 100-200 at 1050 °C and fO_2 near SSO, concluding that fO_2 at sulfide saturation has a pronounced effect on the solubility of Au in basaltic and andesitic melts. However, recent experiments between 1050 and 1250 °C and at P=200 MPa (Beermann et al. 2011) showed that MSS melts to sulfide liquid over this temperature range (e.g., Bockrath et al. 2004). Since the behavior of HSE and gold is strongly controlled by the nature of the sulfide phase present (e.g., Li et al. 1996; Ballhaus et al. 2001; Barnes et al. 2001; Bockrath et al. 2004; Mungall et al. 2005; Li and Audetat 2012), this finding raises the question about the importance of P-T-fO_2 conditions for metal mobility during magma generation and evolution.

In this study we revisit our earlier results by presenting new experimental measurements of Au partitioning between sulfide phases and basaltic silicate melts at 200 MPa in the temperature range 1050 – 1200 °C. We present a revised model of Au behavior during magma generation to take into account the relative importance of SuL and MSS as the restite sulfide phase during mantle melting, and show that melting at relatively low temperature can release Au-rich magmas even in the presence of residual sulfide.

EXPERIMENTAL APPROACH

Silicate melts of basaltic composition (natural basalt from Mt.Etna, Beermann et al. 2011) and ferrobasaltic composition (Skaergaard intrusion, Botcharnikov et al. 2008; synthetic composition SC1 after Toplis and Carroll 1995) were equilibrated with H_2O- and S-bearing fluids and/or S-rich phases at pressure of 200 MPa and temperature in the range from 1050 to 1200°C in Internally Heated Pressure Vessels (IHPV).

Experiments at 1050 °C were conducted in gold capsules that are relatively resistant to the reaction with S using starting material composed of dry glass, elemental S and H_2O. At higher T the starting H_2O-bearing basaltic glass of Mt.Etna or the dry ferrobasaltic glass (+H_2O) were placed with a sulfide phase in containers made of San Carlos olivine within $Au_{80}Pd_{20}$ capsules (following the method described in Beermann et al. 2011).

The basaltic glass from Mt.Etna contained natural concentrations of trace elements and S-bearing phase was added as natural pyrrhotite (provided by J.Schuessler, Schuessler et al. (2007)). The ferrobasaltic glass was doped with trace elements including PGEs and Au using standard ICP-MS solutions; the S-bearing phase added to the glass was synthetic HSE-doped pyrrhotite (~50 μg/g Au; synthesized following the procedure described in Wohlgemuth-Ueberwasser et al. 2007).

The redox conditions were adjusted by the Ar-H_2 gas mixture in the IHPV as controlled by a Shaw-membrane and monitored by the analysis of content and speciation of volatiles and of ferric-ferrous ratio in the quenched glasses. The nominal redox conditions varied from $\log f O_2 = \Delta$FMQ-0.4 to +3.3 (where FMQ is the oxygen fugacity buffered by the fayalite-magnetite-quartz solid assemblage). We note that internal redox reactions involving the olivine containers resulted in fO_2 different from that expected from the redox state imposed by the IHPV in 24-56-hour experiments of Beermann et al. (2011). The exact redox conditions were not determined in the two 86-hour ferrobasaltic experiments; for these we have fO_2 calculated from the imposed fH_2 assuming aH_2O~1 and taking into account the high

S content of the silicate melt (Table 1 in the main text) which points to significant contribution from sulfate.

The quenched run products consisted mainly of H_2O- and S-bearing glass, fluid and sulfide phases. Several basaltic samples at 1050°C (close to liquidus in H_2O-rich basalt) also contained small amounts of olivine, magnetite, clinopyroxene and plagioclase (see Botcharnikov et al. 2011 and Beermann et al. 2011).

ANALYTICAL METHODS

The analytical approaches were reported previously in Botcharnikov et al. (2011) and Beermann et al. (2011) and are briefly reiterated below. Major element concentrations, Ni and S contents were determined using Electron Probe Micro Analysis (EPMA). Water content was evaluated using FTIR spectroscopy or the difference to 100% of the EPMA total. The Au distribution between glasses and solid phases was quantified by laser-ablation inductively coupled plasma mass spectrometry (LA-ICP-MS; Botcharnikov et al. 2011). In this study, we used a 193 nm excimer laser (Coherent GeoLas Pro) with a Zurich Large Volume ablation cell coupled to a quadrupole-based ICP-MS (Agilent 7500cs) at the Institute of Geosciences, CAU Kiel, Germany. In situ-micro-sampling was done with 80 μm pit size and 15 Hz pulse frequency at 10 $J \cdot cm^{-2}$ for silicate glass and with 20-80 μm pit size and 5 Hz pulse frequency at 3 $J \cdot cm^{-2}$ for sulfide phases. Silicate glass (NIST610 with 23.6 μg/g Au) and sulfide (PGE-A, NiS sulfide with 274 μg/g Au, Gilbert et al. 2012) standards were used for the external calibration of the LA-ICP-MS signal. Silicon and nickel analysed by EPMA were used as internal standards for silicate glasses and sulfide phases, respectively. Glasses were analysed using profiles with the movement rate of 3 μm/s, whereas sulfides were analysed using spot analysis. Micronuggets of Au, typical for quenched silicate glasses obtained in high pressure experiments, were considered as experimental artefacts (e.g., Botcharnikov et al. 2010; Jego

et al. 2010; Jego and Pichavant 2012; Zajacz et al. 2012) and filtered out from the LA-ICP-MS spectra.

Small sulfide phases quenched from 1050°C experiments were present as rounded phases with almost homogeneous appearance in BSE images (see Fig.1a). The EPMA analytical data using a focused and defocused beam did not show significant difference for the quenched sulfide phase (MSS) from 1050°C experiments, indicating the presence of a chemically homogeneous phase which could be quenched without phase separation. On the other hand, large sulfide blobs found in experiments at T>1050°C showed obvious quench effects and formation of quench phases (see Fig.1b,c) pointing to the existence of a liquid phase at these experimental conditions (e.g., Mungall et al. 2005). Ni was analysed with EPMA (15 kV, 100 nA beam current, calibrated on NiO) using a defocused 20 μm electron beam to overcome heterogeneity of the quenched sulfide liquid (Fig. 1c). The variation in Ni concentration is < 4%. Thus, the size of the beam was large enough to be representative of the bulk composition of the quench sulfide phase existing at high temperature.

RESULTS AND DISCUSSION

The sulfide phases produced in our experiments at 1050°C were originally interpreted as droplets of quenched sulfide liquid by Botcharnikov et al. (2011) owing to their rounded shapes (Fig.1a). However, the homogeneous texture and composition of the sulfide phase indicate that it is MSS rather than quenched SuL. In contrast, in high-T experiments (above 1050 °C) Energy Dispersive X-ray (EDX) analysis showed qualitatively the presence of oxygen in quench-textured sulfides from high-T experiments (Fig.1b,c), supporting our interpretation that they were oxygen-bearing sulfide liquids at run conditions. The presence of MSS at 1050 °C and of SuL at T > 1050 °C is also in agreement with the phase diagram reported by Bockrath et al. (2004).

Figure 2 compares our measured $D^{\text{sulfide-silicate}}_{\text{Au}}$ with previously published values for both MSS and SuL. It must be noted that the data of earlier studies have been obtained using bulk analytical techniques for the determination of Au concentrations resulting in wide scattering of the data presumably due to contamination by metal micronuggets. The application of laser ablation techniques provides much more reliable results because it allows filtering of micronugget spikes from the spectrum. The spike-free parts of the LA ICPMS spectra should theoretically correspond to the parts of the sample which are free of Au particles, because any tiny metal particle should result in a very strong signal compared with very low (ppb to ppm level) Au concentration in the silicate glass. The absence of micronugget effect for sulfide phases is more difficult to prove because the concentrations of dissolved Au are one to two orders of magnitude higher than that in silicate melts. Based on the precision of the determined Au concentrations and on the reproducibility of the repeated measurements for each individual sample, we assume that any micro/nanonugget effect (if present) on the determined partition coefficients is minimized by the signal filtering and is included in the bulk uncertainty. The validation of this assumption is not trivial and requires additional specific study which is technically quite challenging and is not possible based on the experimental results we have. Thus, for the purposes of this study we postulate that the sulfide-silicate partitioning equilibrium is controlled by Au species dissolved in the sulfide and silicate phases and that this equilibrium is not affected by the presence of micro- or nano-particles of Au in either phase.

The $D^{\text{sulfide-silicate}}_{\text{Au}}$ for MSS-saturated ($D^{\text{MSS-sil}}_{\text{Au}}$) basalts determined in this study varies from 110 to 280, with an average value of 170±78 (n = 4), and is in excellent agreement with our earlier results (Botcharnikov et al. 2011) and the experimental results of Li and Audetat (2012) obtained for systems with different bulk compositions and at much higher P and T (1.5-3 GPa, 1175-1300 °C) where both MSS and sulfide liquid coexisted. The dependence of the partitioning behavior of Au on the redox conditions is not well constrained,

yet. The data obtained using LA ICPMS analysis (this study and the work of Li and Audetat, 2012) show no dependence within uncertainty in the investigated range of fO_2.

Two examples of basaltic melts at 1150 °C and two examples of ferrobasaltic melts at 1100 and 1150 °C are consistent within uncertainty and show $D^{SuL\text{-}sil}_{Au}$ values >1000 (the average value is 2205±485, n = 4). A single low $D^{SuL\text{-}sil}_{Au}$ value of 358±34 was determined for sample S8 equilibrated at 1200 °C. Both the LA-ICPMS spectra for silicate glasses and the spectra for sulfides collected in this sample showed well-reproducible patterns from several analyses, resulting in a relatively low uncertainty. However, although the concentration of Au in the quenched sulfide is similar to that found in other high-T Etna basalt samples, the concentration of Au in the silicate glass is significantly higher, leading us to suppose that there may have been widely dispersed microdroplets of SuL or Au micronuggets within the glass phase, leading to a spuriously low calculated $D^{SuL\text{-}sil}_{Au}$. If this experiment is not considered, then the $D^{SuL\text{-}sil}_{Au}$ values for the systems with SuL are about 20 times higher than the values for MSS-saturated systems, in agreement with the results of Li and Audetat (2012).

The good correspondence between several independent datasets shown in Figure 2, obtained using different experimental methods and analytical laboratories, implies that temperature in the range from 1050 to 1350 °C, pressure in the range from 0.2 bar to 3 GPa, basaltic melt composition and redox conditions in the range from ΔFMQ-3 to ΔFMQ+1.3 do not have decisive effects on $D^{sulfide\text{-}silicate}_{Au}$ in basaltic systems. Rather, the main factor which governs Au partitioning is the nature of the sulfide phase present in the system and, if both MSS and SuL coexist, the relative proportions of these phases (Li and Audetat 2012).

The other key factor controlling the comportment of Au during mantle melting is the solubility of S, as dictated by T, P, melt composition, and fO_2 (e.g., O'Neill and Mavrogenes 2001; Jugo et al. 2005; Liu et al. 2007; Moune et al. 2009; Beermann et al. 2011; Botcharnikov et al. 2011). As predicted by modelling (Moretti and Baker 2008) and demonstrated experimentally (e.g., Beermann et al. 2011; Botcharnikov et al. 2011) we find

that the solubility of S at sulfide saturation in basaltic melts has a positive correlation with fO_2 due to the concomitant increase in fS_2 and fO_2 in the system. Moreover, at the fO_2 corresponding to that of the sulfide-sulfate transition, the solubility of S increases significantly due to the presence of sulfate species with higher solubility than that of sulfide species (e.g., Jugo et al. 2010). Thus, enhanced S solubility observed at the sulfide-sulfate transition may dramatically affect dissolution and extraction of S-bearing phases from mantle rocks during partial melting or the precipitation of S-bearing phases during magma crystallization.

In Figure 3 we present the results of some simple models of non-modal fractional melting of the mantle (according to Shaw 1970) to test the effects of the identity of the restite sulfide phase, temperature and fO_2 on Au distribution between mantle and basaltic melt.

The concentration of Au in the silicate liquid (C_{Au}) representing the instantaneous fractional non-modal melt of the mantle source was modelled by the expression $C_{Au} = C_{oAu}/D_o(1\text{-}PF/D_o)^{(1/P\text{-}1)}$, where C_{oAu} is the bulk concentration of Au in the source prior to melting, D_o is the bulk partition coefficient for the original solid phases before the onset of melting, P is the bulk distribution coefficient of the minerals that produce the melt, and F is the weight fraction of melt produced (see eq.13 in Shaw 1970 for details). Since sulfides have predominant control on Au behavior, D_o and P are dependent on the abundances of sulfides and Au in the source, on the solubility of sulfides in the melt and on $D^{\text{sulfide-silicate}}_{Au}$. We assume that Au is perfectly incompatible with silicate minerals, so that the D_o and P terms depend only on the sulfide/silicate partition coefficient and the fraction of sulfide that enters the silicate melt in the melting reaction (i.e., its solubility). Pooled melts were modeled with the expression $C_{Au} = C_{oAu}/F[1\text{-}(1\text{-}PF/D_o)^{1/P}]$ (eq. 14 in Shaw 1970) with all terms defined as above.

The initial concentration of Au in the mantle is assumed to be about 1 ng/g, and the abundance of S present in the mantle as sulfides is considered to be about 250 μg/g S

(McDonough and Sun 1995; 690 μg/g sulfide, assuming a sulfide phase composed mainly of FeS). The exact S content of the mantle source depends presumably on the tectonic environment, i.e, whether the mantle has been depleted by previous melt extraction or enriched by metasomatic reactions with S-bearing fluids. The depleted mantle that is first encountered by fluids in nascent arcs probably has about 120 ppm S (Salters and Stracke 2004) but then S is added in unknown quantities as arc system evolves (e.g., Mungall 2002, Richards 2009), hence any S concentration can be chosen. Thus, here we use an average S value for pyrolite mantle for simplicity. The variation in the amount of sulfide phase present in the mantle source at given bulk Au content may influence the absolute concentrations of Au in the produced melts but the relative effects of MSS and SuL on the partitioning will not be affected. Higher initial S contents in the mantle will correspond with higher initial modal abundance of the condensed sulfide phase and will require greater degrees of melting before sulfide exhaustion from the restite, but the fundamental control of Au concentration will remain the physical state of the sulfide phase.

The calculations were done for temperature of 1100°C which is at the lower limit of partial melting temperatures for arc magma generation at 1 GPa, that is for the mantle containing certain amount of water and relevant for the stability of MSS (Bockrath et al. 2004). Temperature of 1200°C is relevant for the melting of dry peridotite at 1 GPa where sulfide liquid only is stable. The dissolution reaction of sulfide is constrained by our estimate of the solubility of S in basaltic melt at 1100 and 1200°C using extrapolation and interpolation of experimental data for basalts obtained in the studies of Jugo et al. (2005), Liu et al. (2007), Beermann et al. (2011) and Botcharnikov et al. (2011). The effect of pressure on S solubility in basaltic melts is relatively small (e.g., Mavrogenes and O'Neill 1999; Moune et al. 2009) and assuming isobaric melting we do not consider any pressure effect. The $D^{\text{sulfide-silicate}}_{\text{Au}}$ is assumed to be independent of T, P, fO_2, and melt composition and was taken to be

249 170 and 2200 for MSS and SuL, respectively (average values determined in this study, Table
250 1).

251 Two principal controls are apparent on Au comportment in Figure 3; the identity of the
252 sulfide phase in the restite and the oxidation state at which melting occurs. At 1100 °C all
253 sulfide is present as MSS, which has a low enough $D^{\text{MSS-sil}}_{\text{Au}}$ to allow significant
254 concentration of Au in the melt even while sulfide remains stable in the restite. However at
255 1200 °C sulfide is present in liquid form, with a much larger $D^{\text{SuL-sil}}_{\text{Au}}$. The concentration of
256 Au in basalt is very low while SuL remains in the restite, rising to high values only in the last
257 infinitesimal stages of melting prior to complete sulfide exhaustion. The instantaneous
258 fractional melts approach a singularity at that point before falling to zero Au thereafter,
259 whereas the pooled melts rise to join the curve representing all S-undersaturated melts
260 (including those formed at fO_2 above SSO where sulfide is never a stable restite phase). The
261 significance of the identity of the sulfide phase is that depending on the bulk S content of the
262 mantle Au-rich magmas can form at arbitrarily low degrees of melting if MSS is in the restite,
263 whereas Au-rich magmas in equilibrium with sulfide liquid can only be generated if the
264 degree of melting is sufficient to completely dissolve SuL into the basaltic melt.

265 The second key control on Au in basalts is fO_2, due to the dramatic effect it has on S
266 solubility. High S solubility leads to rapid exhaustion of the sulfide phase from the restite,
267 whether it is MSS or SuL, allowing melt compositions to join the sulfide-absent curve
268 (dashed lines, Fig. 3c, 3d). Whereas more than 8% fractional melting is required to exhaust
269 sulfide from the source at FMQ, the sulfide has been completely dissolved after less than 3%
270 melting at FMQ+1.5.

271 Also shown for comparison in Figure 3 are the compositions of unusually Au-rich
272 alkaline mafic rocks from Hawaii (Sisson 2003), which were produced by small degrees of
273 melting of phlogopite garnet lherzolite at about 1350 °C, 3.0 GPa (Sisson et al. 2009) at
274 ΔFMQ between 0.5 and 1.5. For each sample containing > 10 wt% MgO, the melt fraction F

was calculated using the measured Zr concentrations and assuming that $D_{oZr} = 0.033$ and $C_{oZr} = 8.9$ μg/g (e.g., Sisson et al. 2009) for pooled modal melts (eq. 10 in Shaw 1970). Although the data are rather scattered, it is evident that even the highest Au values reported by Sisson (2003) would be unremarkable if melting occurred in the presence of MSS, whereas some low-degree melts contain an order of magnitude too much Au to have been generated in the presence of residual sulfide liquid. The MSS solidus occurs close to 1350 °C at 3 GPa (Bockrath et al. 2004), lending some support to our inference that the Hawaiian basalts were generated at a temperature below the MSS solidus.

CONCLUSIONS

New experimental and analytical data illustrate that the nature of sulfide phase present in magmatic source during magma generation or evolution exerts a major control on the partitioning of Au between sulfides and silicate melt. Partition coefficients found for systems saturated with monosulfide solid solution (MSS) are at least order of magnitude lower than those observed in systems coexisting with sulfide liquids (SuL), implying that Au-enriched magmas are expected to be formed at lower temperatures or at higher pressures, when MSS is stable. Thus, the predominance of MSS over SL in the source or/and oxidizing conditions close to or above the sulfide-sulfate transition are prerequisite factors governing occurrence of Au-enriched magmas.

ACKNOWLEDGEMENTS

This study was supported by the German Science Foundation (DFG grants Bo2941-1 and 2) and by the Leibniz Universität Hannover. J.Feige is acknowledged for the help with the preparation of olivine containers. The manuscript has been substantially improved by the constructive reviews of M.Pichavant, J.Richards, C.Ballhaus, and I.Swainson. The editorial handling by I.Swainson is also greatly acknowledged.

REFERENCES

Ballhaus, C., Tredoux, M., and Späth, A. (2001) Phase relations in the Fe–Ni–Cu–PGE–S system at magmatic temperature and application to massive sulphide ores of the Sudbury igneous complex. Journal of Petrology, 42, 1911-1926.

Barnes, S.-J., van Achterbergh, E., Makovicky, E., and Li, C. (2001) Proton microprobe results for the partitioning of platinum-group elements between monosulphide solid solution and sulphide liquid. South African Journal of Geology, 104 275-286.

Beermann, O., Botcharnikov, R.E., Holtz, F., Diedrich, O., and Nowak, M. (2011) Temperature dependence of sulfide and sulfate solubility in olivine-saturated basaltic magmas. Geochimica et Cosmochimica Acta, 75, 7612-7631.

Bezmen, N.I., Asif, M., Brugmann, G.E., Romanenko, I.M., and Naldrett, A.J. (1994) Distribution of Pd, Rh, Ru, Ir, Os, and Au between sulfide and silicate metals. Geochimica et Cosmochimica Acta, 58, 1251-1260.

Bockrath, C., Ballhaus, C., and Holzheid, A. (2004) Fractionation of the platinum-group elements during mantle melting. Science, 305, 1951-1953.

Botcharnikov, R.E., Almeev, R.R., Koepke, J., and Holtz, F. (2008) Phase relations and liquid lines of descent in hydrous ferrobasalt - Implications for the Skaergaard Intrusion and Columbia River flood basalts. Journal of Petrology, 49, 1687-1727.

Botcharnikov, R.E., Linnen, R.L., and Holtz, F. (2010) Solubility of Au in Cl- and S-bearing hydrous silicate melts. Geochimica et Cosmochimica Acta, 74, 2396-2411.

Botcharnikov, R.E., Linnen, R.L., Wilke, M., Holtz, F., Jugo, P.J., and Berndt, J. (2011) High gold concentration in sulphide-bearing magma at oxidizing conditions. Nature Geoscience, 4, 112-115.

Crocket, J.H., Fleet, M.E., and Stone, W.E. (1997) Implications of composition for experimental partitioning of platinum-group elements and gold between sulfide liquid and basalt melt: The significance of nickel content. Geochimica et Cosmochimica Acta, 61, 4139-4149.

Fleet, M.E., Crocket, J.H., Liu, M.H., and Stone, W.E. (1999) Laboratory partitioning of platinum-group elements (PGE) and gold with application to magmatic sulfide-PGE deposits. Lithos, 47, 127-142.

Gilbert, S., Danyushevsky, L., Robinson, P., Wohlgemuth-Ueberwasser, C., Pearson, N., Savard, D., Norman, M., and Hanley, J. (2012) A comparative study of five reference materials and the Lombard meteorite for the determination of the platinum-group elements and gold by LA-ICP-MS. Geostandards and Geoanalytical Research, doi: 10.1111/j.1751-908X.2012.00170.x.

Hamlyn, P.R., Keays, R.R., Cameron, W.E., Crawford, A.J., and Waldron, H.M. (1985) Precious metals in magnesian low-Ti lavas: Implications for metallogenesis and sulfur saturation in primary magmas. Geochimica et Cosmochimica Acta, 49, 1797-1811.

Jégo, S., and Pichavant, M. (2012) Gold solubility in arc magmas: Experimental determination of the effect of sulfur at 1000°C and 0.4 GPa. Geochimica et Cosmochimica Acta, 84, 560-592.

Jégo, S., Pichavant, M., and Mavrogenes, J.A. (2010) Controls on gold solubility in arc magmas: An experimental study at 1000 °C and 4 kbar. Geochimica et Cosmochimica Acta, 74, 2165-2189.

Jugo, P.J., Luth, R.W., and Richards, J.P. (2005) An experimental study of the sulfur content in basaltic melts saturated with immiscible sulfide or sulfate liquids at 1300°C and 1.0 GPa. Journal of Petrology, 46, 783-798.

Jugo, P.J., Wilke, M., and Botcharnikov, R.E. (2010) Sulfur K-edge XANES analysis of natural and synthetic basaltic glasses: Implications for S speciation and S content as function of oxygen fugacity. Geochimica et Cosmochimica Acta, 74, 5926-5938.

Li, C., Barnes, S.J., Makovicky, E., Rose-Hansen, J., and Makovicky, M. (1996) Partitioning of nickel, copper, iridium, rhenium, platinum, and palladium between monosulfide solid solution and sulfide liquid: Effects of composition and temperature. Geochimica et Cosmochimica Acta, 60, 1231-1238.

Li, Y. and Audétat, A. (2012) Partitioning of V, Mn, Co, Ni, Cu, Zn, As, Mo, Ag, Sn, Sb, W, Au, Pb, and Bi between sulfide phases and hydrous basanite melt at upper mantle conditions. Earth and Planetary Science Letters, 355–356, 327-340.

Liu, Y., Samaha, N.-T., and Baker, D.R. (2007) Sulfur concentration at sulfide saturation (SCSS) in magmatic silicate melts. Geochimica et Cosmochimica Acta, 71, 1783-1799.

Mavrogenes, J.A. and O'Neill, H.S.C. (1999) The relative effects of pressure, temperature and oxygen fugacity on the solubility of sulfide in mafic magmas. Geochimica et Cosmochimica Acta, 63, 1173-1180.

McDonough, W.F. and Sun, S.-s. (1995) The composition of the Earth. Chemical Geology, 120, 223-253.

Moretti, R. and Baker, D.R. (2008) Modeling the interplay of fO_2 and fS_2 along the FeS-silicate melt equilibrium. Chemical Geology, 256, 286-298.

Moune, S., Holtz, F., and Botcharnikov, R. (2009) Sulphur solubility in andesitic to basaltic melts: implications for Hekla volcano. Contributions to Mineralogy and Petrology, 157, 691-707.

Mungall, J.E. (2002) Roasting the mantle: Slab melting and the genesis of major Au and Au-rich Cu deposits. Geology, 30, 915-918.

Mungall, J.E., Andrews, D.R.A., Cabri, L.J., Sylvester, P.J., and Tubrett, M. (2005) Partitioning of Cu, Ni, Au, and platinum-group elements between monosulfide solid solution and sulfide melt under controlled oxygen and sulfur fugacities. Geochimica et Cosmochimica Acta, 69, 4349-4360.

Mungall, J.E., Hanley, J.J., Arndt, N.T., and Debecdelievre, A. (2006) Evidence from meimechites and other low-degree mantle melts for redox controls on mantle-crust fractionation of platinum-group elements. Proceedings of the National Academy of Sciences, 103, 12695-12700.

O'Neill, H.S.C. and Mavrogenes, J.A. (2002) The sulfide capacity and the sulfur content at sulfide saturation of silicate melts at 1400°C and 1 bar. Journal of Petrology, 43, 1049-1087.

Richards, J.P. (2009) Postsubduction porphyry Cu-Au and epithermal Au deposits: Products of remelting of subduction-modified lithosphere. Geology, 37(3), 247-250.

Salters, V.J.M., and Stracke, A. (2004) Composition of the depleted mantle. Geochemistry Geophysics Geosystems, 5.

Schuessler, J.A., Schoenberg, R., Behrens, H., and Blanckenburg, F.v. (2007) The experimental calibration of the iron isotope fractionation factor between pyrrhotite and peralkaline rhyolitic melt. Geochimica et Cosmochimica Acta, 71, 417-433.

Sisson, T.W. (2003) Native gold in a Hawaiian alkalic magma. Economic Geology, 98, 643-648.

Sisson, T.W., Kimura, J.-I., and Coombs, M.L. (2009) Basanite-nephelinite suite from early Kilauea: carbonated melts of phlogopite-garnet peridotite at Hawaii's leading magmatic edge. Contributions to Mineralogy and Petrology, 158, 803-829.

Shaw, D.M. (1970) Trace element fractionation during anatexis. Geochimica et Cosmochimica Acta, 34, 237-243.

Solomon, M. (1990) Subduction, arc reversal, and the origin of porphyry copper-gold deposits in island arcs. Geology, 18, 630-633.

Stone, W.E., Crocket, J.H., and Fleet, M.E. (1990) Partitioning of Palladium, Iridium, Platinum, and Gold between Sulfide Liquid and Basalt Melt at 1200-Degrees-C. Geochimica et Cosmochimica Acta, 54, 2341-2344.

Toplis, M.J., and Carroll, M.R. (1995) An experimental study of the influence of oxygen fugacity on Fe-Ti oxide stability, phase relations, and mineral-melt equilibra in ferro-basaltic systems. Journal of Petrology, 36, 1137-1170.

Wohlgemuth-Ueberwasser, C., Ballhaus, C., Berndt, J., Stotter nee Paliulionyte, V., and Meisel, T. (2007) Synthesis of PGE sulfide standards for laser ablation inductively coupled plasma mass spectrometry (LA-ICP-MS). Contributions to Mineralogy and Petrology, 154, 607-617.

Zajacz, Z., Candela, P.A., Piccoli, P.M., Wälle, M., and Sanchez-Valle, C. (2012) Gold and copper in volatile saturated mafic to intermediate magmas: Solubilities, partitioning, and implications for ore deposit formation. Geochimica et Cosmochimica Acta, 91, 140-159.

FIGURE CAPTIONS

Figure 1. Back-scattered electron images illustrating the appearance of sulfide phases in experiments at 1050°C (a) and 1150°C (b,c). (a) Sulfide, olivine and silicate melt phases in the experimental product from run 0-15-2-red (Table 1). The sulfide phase is monosulfide solid solution (MSS). The MSS is commonly in direct contact with olivine (OL) and fluid bubbles (black) pointing to nucleation and equilibration processes during the experiment. (b) Experimental product from experiment S19 illustrating coexistence of sulfide liquid, fluid bubble, silicate melt and olivine container. Sulfide liquid experienced quench modifications as evident from detail view in (c) representing the area outlined by the dashed line in panel (b).

Figure 2. Partition coefficients of Au between sulfide phases and silicate melt. Grey symbols represent literature data for the systems with sulfide liquid (St90 is after Stone et al., 1990; Be94 is after Bezmen et al., 1994; Cr97 is after Crocket et al., 1997; Fl99 is after Fleet et al., 1999; Li12 is after Li and Audetat, 2012); open circles are the data of Li and Audetat (2012) for the partitioning between MSS and silicate. Black squares and open triangles are the data from this study for SuL/silicate and MSS/silicate coefficients, respectively.

Figure 3. The model of Au extraction in an instantaneous fractional melt during melting of the mantle containing 1 ng/g Au and 250 μg/g S. The model takes into account the redox conditions, the degree of partial melting (F) and the nature of sulfide phase present: (a) for MSS at 1100°C and (b) for sulfide liquid at 1200°C. The grey rectangles illustrate the redox conditions and the range of Au concentrations in bulk rocks for basanitic magmas from Kilauea (Sisson, 2003). The solid vertical lines define the stability field of sulfides as a function of fO_2. The long-dashed lines show the expected concentration of Au in the oxidized melts with 5% melting at complete sulfide exhaustion. Panels 3c and d show the dependence of melt Au on degree of melting at various oxygen fugacities, showing both instantaneous (short-dashed lines) and pooled (solid) fractional melts; dashed lines show the compositions of melts produced after sulfide exhaustion either due to melting above the SSO buffer or due to complete dissolution of sulfide in the silicate melt. Since a condensed sulfate phase does not form until S concentrations reach approximately 1% in the melt, we neglect sulfate phases in our restite assemblage, assuming that all S in the mantle assemblage is either MSS or SuL. Black dots are the data on Au content in basanitic magmas (see text).

449 Table 1. Experimental conditions at P=200 MPa and analytical results.
450

Run	S6 *	S36 *	S41 *	0-15-2-red §	BOL6	S19 b	S20 §	BOL5	S8 §
T, °C	1050	1050	1050	1050	1100	1150	1150	1150	1200
logfO_2	-9.2	-10.1	-10.5	-9.7	-8.1 **	-8.4	-8.6	-8.0 **	-7.8
ΔFMQ	0.9	-0.1	-0.4	0.3	1.3 **	0.3	0.1	0.7 **	0.3
S in melt, μg/g	2760±60	1250±60	710±40	1200±100	8190±350	3100±600	2700±700	6110±260	3000±400
H_2O in melt, wt%	4.5	4.3	2.7	4.8	4.6	3.2	3.1	2.8	3.4
Fe in sulfide, wt%	59.59±0.24	61.43±0.34	62.21±0.49	60.87±0.40	58.73±0.54	60.35±0.59	60.33±1.03	55.61±0.76	59.78±0.73
S in sulfide, wt%	41.01±0.28	38.14±0.22	37.76±0.17	38.76±0.19	34.49±0.84	34.26±0.33	33.98±0.33	35.67±1.23	34.66±0.59
Ni in sulfide, μg/g	n.d.	1254±130	818±61	1734±367	11498±304	6152±144	4639±163	27192±817	5377±142
Au in melt, μg/g	7.97±0.03	2.96±0.22	0.91±0.12	13.04±2.61	0.22±0.05	0.76±0.16	0.52±0.10	0.38±0.08	6.096±0.309
Au in sulfide, μg/g	1431±103	326±186	253±110	1499±328	371±64	2098±174	1268±45	737±98	2185±176
D_{Au} sulfide/silicate	179±13	110±63	278±126	115±34	1694±467	2764±607	2438±464	1924±468	358±34
D_{Au} MSS average		170±78							
D_{Au} SuL average						2205±485			

451 Notes:
452 n.d. - not determined;
453 * - samples from Botcharnikov et al. (2011), reanalysed for sulfide composition;
454 § - samples from Beermann et al. (2011), reanalysed for sulfide composition and for Au
455 concentrations in sulfides and silicate melt;
456 ** - redox conditions were estimated from the conditions imposed by Ar-H_2 mixture of the
457 IHPV.
458

459

460

461

462

463

464

465

466

467

468

469

470

471

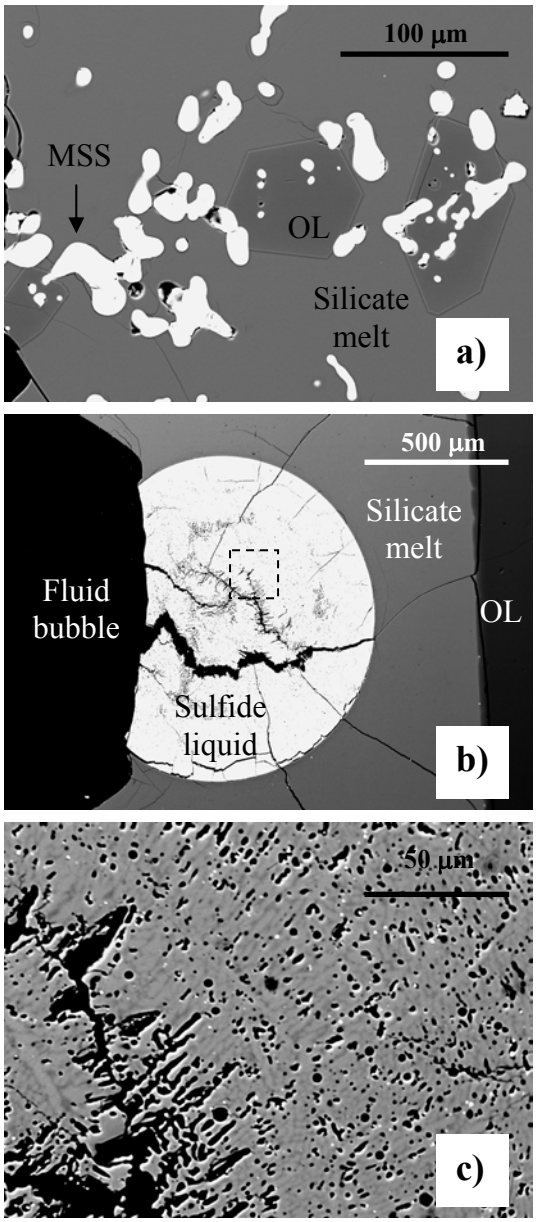

Figure 1. Botcharnikov et al.

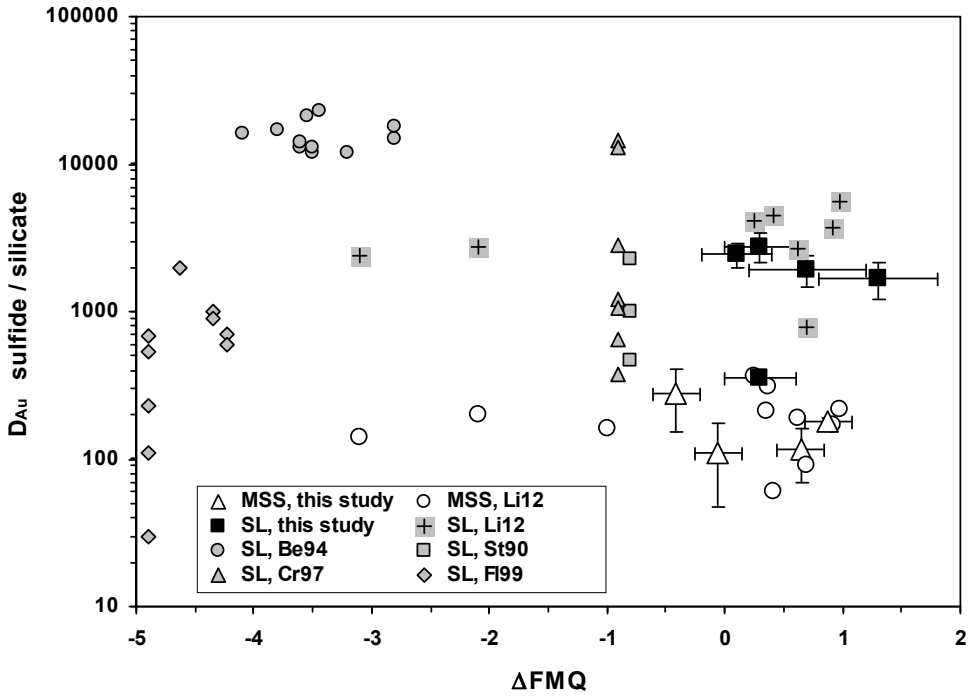

Figure 2. Botcharnikov et al.

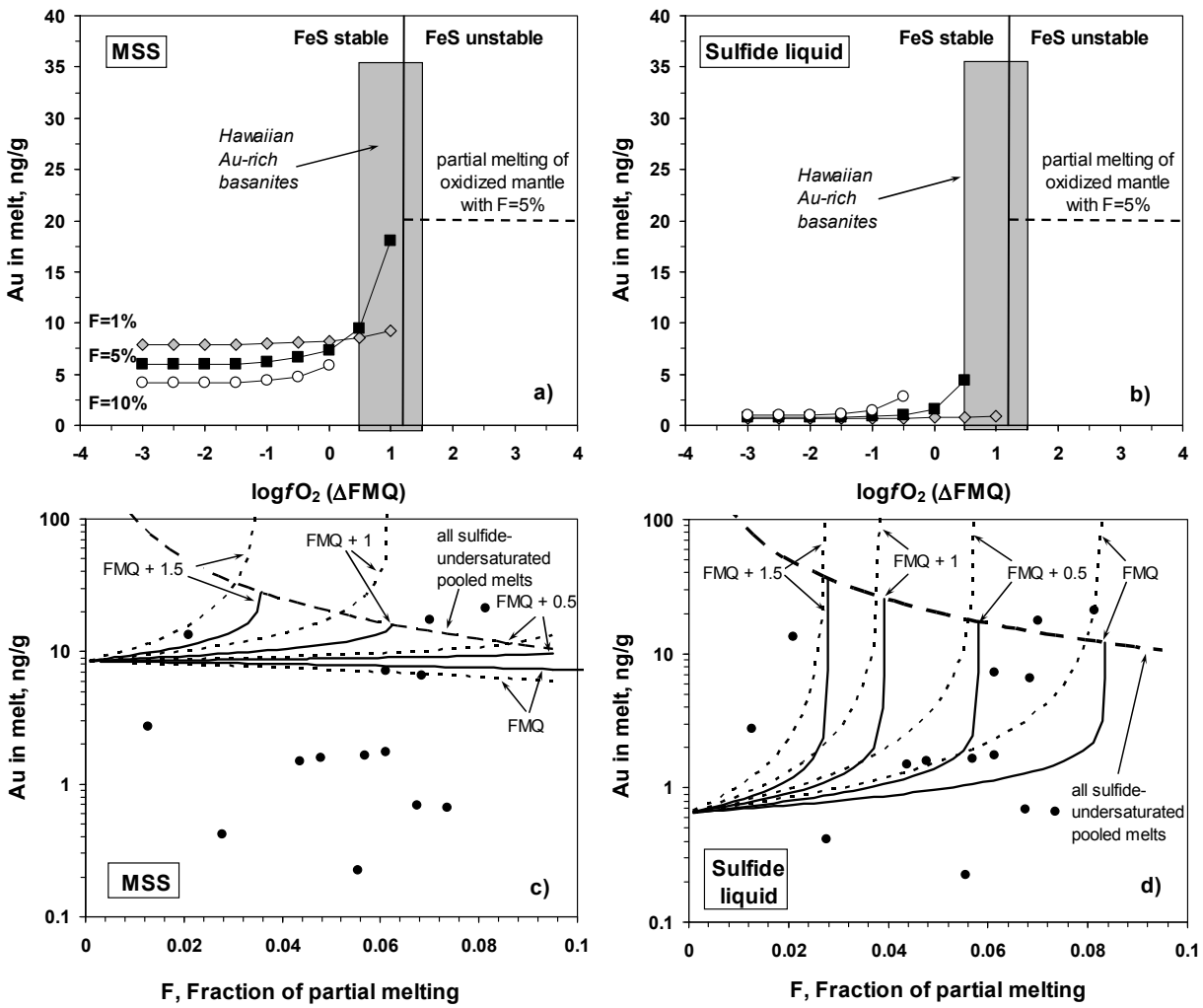

Figure 3. Botcharnikov et al.